1994

Monte Carlo simulation of acetonitrile clusters [CH3CN] N , N=2–256: Melting transitions and even/odd character of small clusters (N=2–9), heat capacities, density profiles, fractal dimension, intracluster dimerization, and dipole orientation

D. Wright
Virginia Commonwealth University

M. Samy El-Shall
Virginia Commonwealth University, mselshal@vcu.edu

Wright D., and El-Shall, M. S. Monte Carlo simulation of acetonitrile clusters [CH3CN] N , N=2–256: Melting transitions and even/odd character of small clusters (N=2–9), heat capacities, density profiles, fractal dimension, intracluster dimerization, and dipole orientation. The Journal of Chemical Physics, 100, 3791 (1994).

Monte Carlo simulation of acetonitrile clusters $[CH_3CN]_N$, $N=2$–256: Melting transitions and even/odd character of small clusters ($N=2$–9), heat capacities, density profiles, fractal dimension, intracluster dimerization, and dipole orientation

D. Wright and M. Samy El-Shall[a)]
Department of Chemistry, Virginia Commonwealth University, Richmond, Virginia 23284-2006

(Received 2 August 1993; accepted 19 November 1993)

The thermodynamic and structural properties of acetonitrile clusters $[CH_3CN]_N$, $N=2$–15, 20, 30, 60, 128, and 256 have been investigated using Monte Carlo simulation. Interactions in the small clusters ($N \leqslant 9$) are dominated by antiparallel pairing of the molecular dipoles. The simulations reveal rigid $\leftrightarrow$ fluid (melting) transitions with a remarkable even–odd alternation in the transition temperatures for the $N=2$–9 clusters. The higher melting temperatures of the even-N clusters arise as consequences of the antiparallel paired dipoles which provide favorable electrostatic interactions. Even–odd alternation has also been observed in the configurational energies and heat capacities and the percentage of molecules possessing an antiparallel nearest neighbor. These observations are consistent with the fact that Coulomb potential terms dominate the interaction energies in clusters with $N < 12$. The average density in clusters with $N > 60$ is fairly well represented by the bulk liquid density. Order parameters characterizing dipole orientation indicate that the molecular dipoles tend to lie flat on the cluster surface for $N \geqslant 30$. Significant dimerization within the clusters suggests evaporation of molecules via dimers and an enhancement of evaporative loss over condensation and this may explain the slower nucleation rates observed for acetonitrile compared to the predictions of the classical nucleation theory.

I. INTRODUCTION

Acetonitrile is a highly polar aprotic molecule with a dipole moment of 3.9 D.[1] It plays an important role as a common solvent in a wide variety of chemical syntheses, reactions and processes with many applications in liquid chromatography, electrochemistry, and atmospheric chemistry.[2–5] The bulk liquid has an oriented structure with a short range order as determined from both neutron scattering and x-ray studies.[6–8] Structural and dynamic properties, as inferred from nuclear magnetic resonance (NMR),[9] IR,[10], and Raman[11] spectroscopic studies, have shown the significance of dipole–dipole interaction in determining short range molecular orientation in the bulk liquid and solid. In the perfectly ordered crystal (216.9 $K < T < T_{mp} = 229$ K) each head-to-tail chain of molecular dipoles ($\rightarrow$) is surrounded by four chains running antiparallel to it, in a monoclinic structure.[1,12] A number of spectroscopic and x-ray studies[13] have suggested the existence of a low temperature solid phase below 216.9 K. The structure of this phase has recently been determined as orthorhombic with eight molecules in a unit cell, exhibiting a strong tendency for head-to-head parallel arrangements.[14]

Extensive theoretical models and computer simulations[15–19] have been utilized to characterize the liquid structure of acetonitrile. In Monte Carlo simulation at temperatures as high as 343 K ($T_{bp} = 354.8$ K), Jorgensen[16] has observed the persistence of head-to-tail chains as well as the tendency for nearest neighbors to lie antiparallel to each other. Both the OPLS[16] (optimized potential for liquid simulation) and Bohm[17] potential models for acetonitrile give the antiparallel configuration as the minimum energy structure for the dimer, and such structures have been observed in diffraction studies of small aggregates in liquid matrices.[20] Far IR spectroscopy of acetonitrile embedded in an inert gas matrix showed the expected bands associated with intermolecular vibrations of the antiparallel dimers.[21] The IR-photodissociation profiles of small acetonitrile clusters[22,23] have been interpreted in terms of solidlike clusters with an internal temperature of < 120 K, and further studies by Buck *et al.*[24,25] suggest that clusters with an odd number of molecules should dissociate more easily than those with an even number of molecules due to the stability of the antiparallel configuration for a pair of molecules. They observed distinguished differences in the frequencies and line shapes of the even and odd clusters with the features associated with the even clusters first appearing in the tetramer spectrum and continuing up to the octamer and it was concluded that the octamer ($N=8$) behaves like an odd cluster.[25] In an attempt to relate this even/odd behavior to the low temperature/high temperature solid phases known for bulk acetonitrile, Buck noticed that the odd clusters are in apparent better agreement with the high temperature solid phase.[25] However, the resolved structure observed for the low temperature phase was not reproduced by the spectra of the even clusters. Buck, therefore, suggested that the even clusters may represent a special configuration not found in the condensed phase. It is clear that calculations are needed in order to examine these considerations.

a)To whom correspondence should be addressed.

Recent experiments in our laboratory[26,27] have shown that the homogeneous nucleation of liquid droplets of acetonitrile, as well as other polar compounds such as nitromethane, benzonitrile and nitrobenzene, is not well described by the classical nucleation theory, and that the theory apparently does not take proper account of dipole–dipole interaction in small clusters of highly polar molecules. The experimentally observed rates of nucleation could be accounted for by either of the two following proposals.[28] First, if the surface dipoles orient themselves at the planar and spherical interfaces in a perpendicular fashion with respect to the surface, this would involve an increase in the surface free energies of the critical clusters which would result in slower nucleation rates compared to the predictions of the classical theory. The second proposal involves departure from the usual assumption of a spherical cluster shape by allowing the clusters to have prolate spheroidal shapes which could be forced by favorable head-to-tail and antiparallel alignments of the dipoles both at the surface and in the interior of the cluster. The elongation of the clusters leads to larger surface areas and therefore to an increase in the surface free energies. These two proposals involve very different structural pictures for the critical clusters and could be examined in detail, at least in principle, by computer simulation of the nucleation process within a uniform supersaturated vapor. However, because of the unstable nature of the critical clusters, direct simulations of their average properties including structures and free energies under realistic experimental conditions would be a rather difficult task to achieve. Clearly, several problems must be satisfactorily solved before a complete molecular approach to the nucleation of polar molecules can be directly examined in computer simulation. In this connection, we mention in particular the recent work of Reiss *et al.*[29,30] who presented a new concept defining a cluster existing in unstable material equilibrium but stable mechanical equilibrium with the surrounding vapor. This approach coupled with computer simulation should prove very useful in studying the nucleation of other more complicated systems, in addition to the extensively studied Lennard-Jones systems.

On the other hand, simulations of the thermodynamic, structural and dynamic properties of *isolated* clusters have provided new insights into size effects in large finite systems and on the transition from molecular to macroscopic systems.[31–52] Much of the work has focused on atomic clusters[31–42,50,52] and rare gas clusters containing a molecular chromophore[45,49] but the simulation of molecular clusters, particularly polar ones, has received little attention. Among the few molecular systems studied are benzene (N =2–7, 12–14),[48,53] TeF_6 (N=128),[51,54] CCl_4 (N=225),[55] CO_2(N=2–7,13),[56] and extensive work on H_2O clusters,[57–66] including the most recent work of Wales *et al.*[66] where the techniques developed with atomic clusters for the study of melting and coexistence phenomena were applied to $(H_2O)_8$ and $(H_2O)_{20}$. Simulation methods have also been used to calculate the vibrational spectra of HF (N=2–8),[67] CH_3CN (N=4),[22] and CO_2 (Ref. 68) clusters.

The work reported in this paper involves a systematic investigation of acetonitrile clusters in the size range N=2–256, and of the bulk liquid. Our main emphasis is on how the strong dipole–dipole interaction observed in the bulk liquid and solid will be manifested in small and large clusters, and whether this interaction is capable of inducing rigid or nonrigid structures in clusters of different sizes. A major objective of this study is to characterize the melting transitions in small acetonitrile clusters and to examine the correlation between such transitions and the extent of dipole–dipole interaction. Other questions addressed include whether the dipoles will exhibit a preferential surface orientation, and how dipolar forces will affect the cluster growth pattern.

The outline of the paper is as follows. In Sec. II we give the computational details. Section III considers the configurational energies and heat capacities and in Sec. IV structures of arbitrarily selected equilibrated configurations and the cluster growth pattern are examined. Section V reports the density profiles and order parameters characterizing dipole orientation and in Sec. VI we examine the melting transitions for the N=2–9 clusters. Finally, we conclude this paper in Sec. VII with a summary and discussion of several issues, including implication of the results for the homogeneous nucleation of acetonitrile.

II. COMPUTATIONAL ASPECTS

A. Monte Carlo method

The cluster calculations for $[CH_3CN]_N$, N=2–15, 20, 30, 60, 128, and 256 were carried out using standard Metropolis sampling in the canonical ensemble.[69,70] Initial configurations for the clusters were excised from a bulk liquid sample at 240 K and thoroughly equilibrated at 120 K. For each N, at least two 2.5×10^7 configuration runs were made and for $N>15$ runs of 5×10^7 configurations were also made, mostly on account of the slower convergence of the heat capacities. The main set of runs was made at T=120 K where the clusters were liquidlike in their intermolecular motion (except for N=256) as indicated by the Lindemann index (see below). At this temperature restraining shells were not needed and no evaporation was observed during the reported runs.

For the melting transition study a series of runs for each cluster size (N=2–9) was obtained by slowly cooling (or heating) in 10 or 20 K intervals, with usually more than 5×10^6 configurations of equilibration at each temperature. For $N\geqslant5$ and near the transition temperature, runs with as many as $(1–2.5)\times10^8$ configurations were necessary for satisfactory convergence of the Lindemann index. The maximum displacement and rotation of a monomer were kept fixed during the melting transition study giving an average acceptance ratio of about 30% (smaller at low T, higher at high T).

The bulk liquid was also simulated at T=120 K using 128 monomers in a cubic cell and other standard procedures including periodic boundary conditions and cutoff corrections to the energy[70] (Lennard-Jones terms only) for the potential truncation. The sample was first equilibrated

at 343 K (1 atm), cooled to 240 K (1 atm) (about 10 K above the bulk freezing point), and then cooled in 40 K intervals to 120 K where it was equilibrated for 2×10^7 configurations and volume changes were attempted every 500 configurations. After two 5×10^6 configuration runs at 120 K (1 atm) the system density was set to the average value obtained over the two runs, the potential extended to exactly half the box length and the system further equilibrated in the NVT ensemble. The final results for the energy and heat capacity were obtained from the final 2.5×10^7 configurations run in the NVT ensemble. For all of these runs the maximum displacement and rotation of a monomer were set at 0.15 Å and 22°, respectively, giving acceptance ratios of 18%–25%. All runs were divided into segments of 10^6 configurations and standard deviations were calculated[71] using either

$$\sigma_1^2=\sum_i^m (x_i-\bar{x})^2/m(m-1) \text{ or } \sigma_2^2=\sum_i^m (x_i-\bar{x})^2/m,$$

where x_i is the average value of x over a 10^6 configuration segment of a run, $\bar{x}$ is the average of x_i over the entire run and m is the total number of segments into which the run was divided. Subsequent to the completion of our original simulations, additional runs using two other differently organized codes (including a derivative of Jorgensen's MCLIQ program) confirmed the results reported here.

B.The OPLS potential function

The OPLS potential function for rigid acetonitrile molecules developed by Jorgensen[16] was used in the simulations. It consists of a Lennard-Jones+Coulomb (12-6-1) potential centered on each of the CH_3, C, and N sites. It assumes the total cluster or bulk energy to be pairwise additive and each pairwise interaction is of the form

$$\Delta e_{ab}=\sum_i^{\text{on}a}\sum_j^{\text{on}b}\left(\frac{q_iq_je^2}{r_{ij}}+\frac{A_{ij}}{r_{ij}^{12}}-\frac{C_{ij}}{r_{ij}^{6}}\right), \quad (1)$$

where Δe_{ab} is the interaction energy between two molecules a and b, and the A_{ij} and C_{ij} can be expressed in terms of Lennard-Jones (LJ) σ's and ϵ's as $A_{ii}=4\epsilon_i\sigma_i^{12}$ and $C_{ii}=4\epsilon_i\sigma_i^6$. The q_i are the partial charges assigned to each site and e is the magnitude of the electron charge. Standard bond lengths and angles based on microwave structures are assumed and the OPLS model parameters can be found in Ref. 16. The average errors in the computed bulk properties of acetonitrile using the OPLS potential are 1%–2%(298–343 K).[16] For comparison, the more explicit six-site model of Bohm *et al.*[17] and the three-site model of Edwards *et al.*[72] give 6% and 12% errors, respectively. The Bohm potential gives a somewhat better dipole moment (Bohm—4.14 D, OPLS—3.44 D, expt.—3.92 D) but due to the rather large clusters involved in this study and the rather long runs needed the OPLS potential was used. As noted by Jorgensen,[16] this potential model can be evaluated four times faster than the Bohm model, while still yielding excellent results for the liquid's properties.

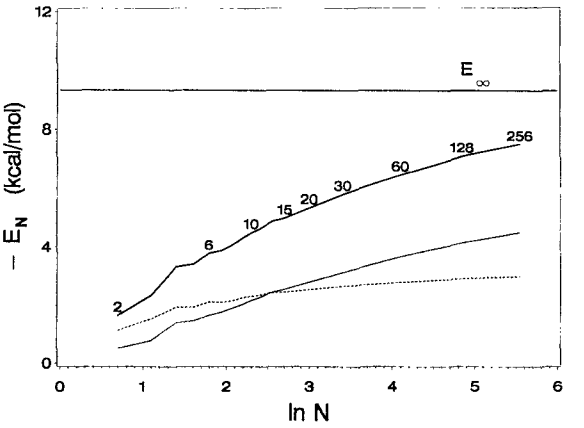

FIG. 1. Average configurational energy per molecule in a cluster of size N for $[CH_3CN]_N$ at 120 K (heavy solid line). The dashed line is the Coulomb potential terms only and the light solid line is the LJ terms. The bulk value at 120 K is shown as a horizontal line. Error bars (σ_2's over multiple (2–5) runs of $(2.5–10.0)\times10^7$ configurations are less than the thickness of the lines.

III. ENERGIES AND HEAT CAPACITIES

Figure 1 compares the cluster configurational energy per molecule with the corresponding bulk value at 120 K. The contributions of the Coulomb and LJ terms to the total energy are also shown in Fig. 1. The energy per molecule is a monotonic increasing function of N ranging from 18% of the bulk value at $N=2$ to 79% of the bulk value at $N=256$ and for $N<12$ the dipole–dipole interaction accounts for more than 50% of the total energy. Also important in Fig. 1 are the plateaus observed for $N=2$–7, revealing that the average binding energy per molecule increases more sharply in going from an odd-N cluster to $N+1$ than from an even-N cluster to $N+1$. This effect is attributed to favorable dipole–dipole interactions in the even-N clusters. For example, the contributions of the Coulomb terms to the interaction energies of $N=4$ and $N=5$ are similar (-1.94 kcal/mol) and the increased energy from $N=4$ to $N=5$ is entirely due to LJ terms (-1.37 kcal/mol for

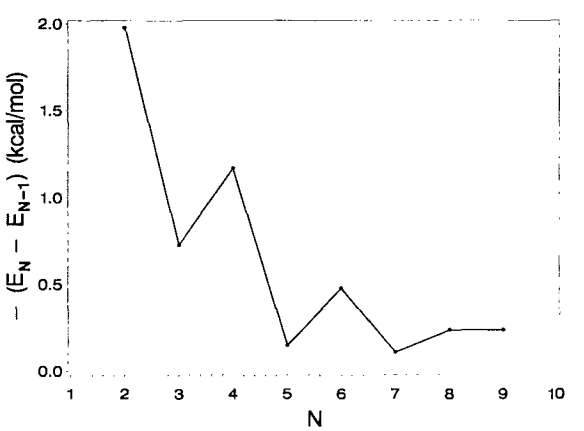

FIG. 2. Change in the average configurational energy per molecule going from a cluster of size $N-1$ to size N for $[CH_3CN]_N$ at 1 K.

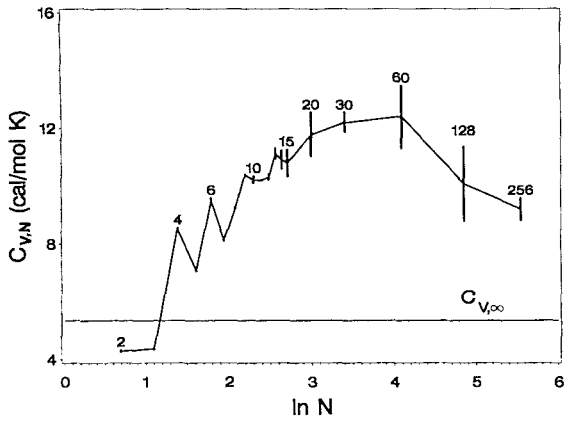

FIG. 3. Average configurational heat capacity per molecule in a cluster of size N for $[CH_3CN]_N$ at 120 K (solid line). The bulk value is shown as a horizontal line. Error bars are σ_2's for the average over multiple (2–5) runs of $(2.5–10.0)\times10^7$ configurations.

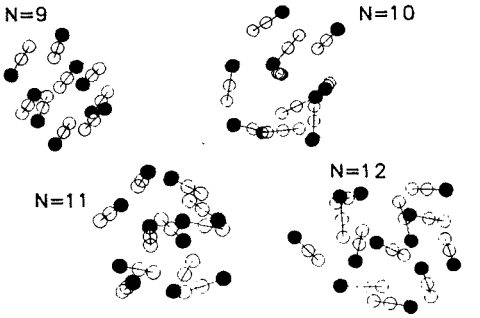

FIG. 5. Stereoplots for $[CH_3CN]_N$, $N=9$–12 at 120 K. Filled circles represent the CH_3 groups.

$N=4$ and -1.46 kcal/mol for $N=5$). A similar result is found in comparing the energies of the $N=6$ and $N=7$ clusters. This feature is highlighted in Fig. 2 where the difference in the configurational energy per molecule ($\Delta E = E_N - E_{N-1}$) is plotted vs N at 1 K and the even/odd character within $N\leqslant9$ is evident. This finding is consistent with the structures and melting transitions to be discussed in Secs. IV and VI, respectively.

Configurational heat capacities were calculated in the standard way from fluctuations in the energy in the canonical ensemble according to

$$C_V=\frac{\langle E^2\rangle-\langle E\rangle^2}{NRT^2}. \tag{2}$$

The cluster heat capacities in the $N=2$–256 range are plotted as a function of N at 120 K (where all the clusters are liquidlike except for $N=256$) in Fig. 3 along with the corresponding bulk value. Two interesting features in Fig. 3 deserve comment. First, the heat capacities rise from below the bulk value at small N, reach a maximum between $N=30$ and $N=60$, and then fall off, suggesting convergence to the bulk from above. A similar trend has also been observed for methanol clusters in this size range[78] and this trend is probably a rather general result. The rapid increase in heat capacity with increasing N at smaller sizes results from the rapid increase in cluster energy per molecule and the rapid increase in the number of available isomers which results in greater frequency of isomerization and consequently, greater fluctuations in the energy. At larger N, the heat capacities tend to decrease since the rate of increase in the energy per molecule decreases and also due to the $N^{-1/2}$ dependence of fluctuations ($N^{-1/2}$ is twice as large for $N=60$ as for $N=256$). The net result is an interior maximum in the C_v vs N plot which appears around $N=30$–60 as indicated in Fig. 3. Hoare and Pal[73] have observed an interior maximum in the calculated vibrational heat capacities of small rigid argon clusters within the harmonic–oscillator approximation. With this model the vibrations are actually interparticle motions determined by the interatomic (LJ) potential, and thus the analogy with intermolecular configurational heat capacities may be reasonable. The second significant feature in Fig. 3 is the even/odd alternation in the heat capacities of the small clusters with $N=3$–8. The even clusters have larger heat capacities than the odd ones and this result arises as a consequence of the pairing of molecules due to favorable dipole–dipole interactions. Evidence in support of this view is presented and discussed in Sec. IV.

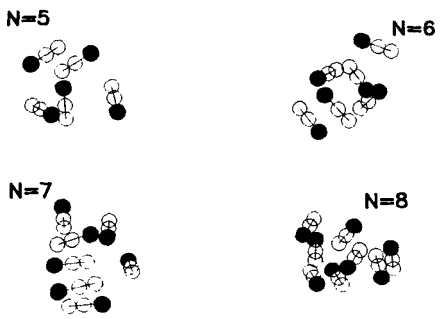

FIG. 4. Stereoplots for $[CH_3CN]_N$, $N=5$–8 at 120 K. Filled circles represent the CH_3 groups.

IV. STRUCTURES AND FRACTAL DIMENSION

To illustrate the growth pattern of acetonitrile clusters, as well as their individual structures, a set of arbitrarily selected equilibrated configurations at 120 K was stereoplotted as shown in Figs. 4–7. The tendency for molecules to exist in antiparallel and displaced parallel dimers is clearly visible even at this very liquidlike temperature (120 K), as is most apparent in the smaller clusters ($N\leqslant15$).

To quantify this pairing into dimers, the fraction of molecules possessing an antiparallel nearest neighbor was calculated for each cluster size. Several criteria were selected as possible definitions for such a neighbor. To be counted as an antiparallel nearest neighbor the separation of the nitrile carbons of a pair of molecules had to be less than the distance R_c, where two values of R_c were used: 4.0 and 4.5 Å. In addition, the angle between the molecular axes had to be between θ_c and 180°, where three values of

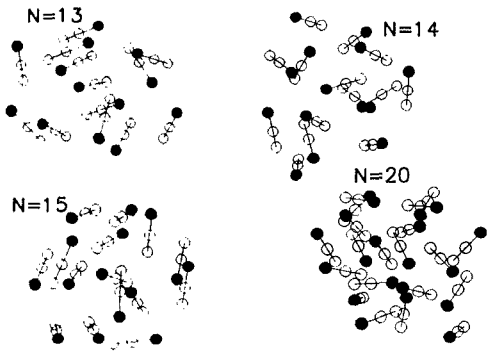

FIG. 6. Stereoplots for $[CH_3CN]_N$, $N=13$–15 and 20 at 120 K. Filled circles represent the CH_3 groups.

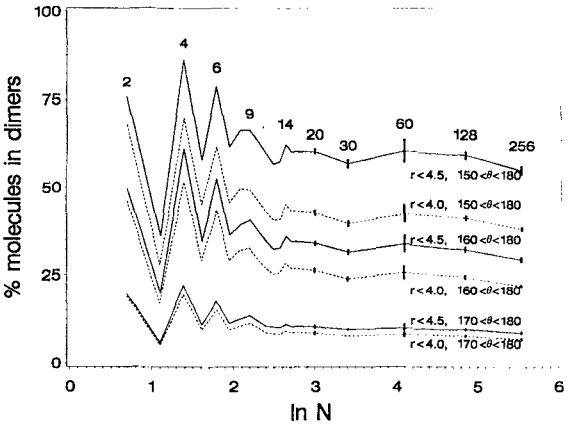

FIG. 8. Percent molecules in $[CH_3CN]_N$ having an antiparallel nearest neighbor vs N at 120 K for various dimer definitions. Error bars ($N\geqslant 20$) are σ_2's for the averages over multiple (2–4) runs of 1.0–$10.0)\times 10^7$ configurations.

θ_c were used: 150°, 160°, and 170°. Every 10 000 configurations each molecule in the cluster was checked for such neighbors which satisfy a given set of criteria. If a molecule happened to have more than one such neighbor, each such neighbor was counted. At the end of the simulation the total number of all such neighbors counted was normalized by the total number of molecules and the number of samples to give an average value for the fraction of molecules possessing an antiparallel nearest neighbor. The results at 120 K, shown in Fig. 8, clearly indicate the importance of dipole–dipole interaction in these clusters. Using the least strict dimer definition ($R_c=4.5$ Å, $\theta_c=150°$) the percentage varies from 54% ($N=256$) to 86% ($N=4$). Although the magnitude of these percentages is strongly dependent upon the choice of dimer definition, the trend with respect to N is independent of this choice. For $N=2$–9, there is a marked oscillation in the percentages, and this can be associated with the even–odd trends at small N already observed in the energies and heat capacities. This feature will have a significant impact on the melting transitions of the smaller clusters as will follow from the discussion in Sec. VI.

To examine the degree of compactness and growth pattern of the clusters we calculated the fractal dimension D_f from the relation[74]

$$R_N=AN^{1/D_f}, \tag{3}$$

where A is a constant and R_N is a measure of cluster radius, taken as the root-mean-square distance between the molecules, which is given by[74]

$$R_N=\left\langle\left(\sum_{i}^{N-1}\sum_{j>i}^{N}\frac{r_{ij}^2}{N(N-1)}\right)^{1/2}\right\rangle, \tag{4}$$

where the intermolecular distances, r_{ij}, were taken as the separations of the molecular centers of mass. Figure 9 shows the size dependence of R_N at $T=120$ K which gives $D_f=3.10$ when all sizes ($N=2$–256) are included in the regression ($\ln N$ vs $\ln R_N$) and $D_f=3.03$ when only $N=20$–256 are included.

The fractal dimension for LJ particles has been found by Gregory and Schug[74] and Heyes and Melrose[75] to be in the range of $D_f=2.3$–2.5 and for Stockmayer molecules Schug[76] has obtained a value of about 2.5. These values were obtained for clusters in equilibrium with vapor. Our result for D_f for acetonitrile clusters is significantly greater than those for LJ and Stockmayer particles and this is probably due to the lower temperature of our simulations.

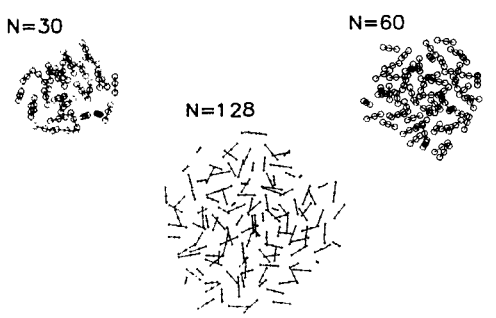

FIG. 7. Stereoplots for $[CH_3CN]_N$, $N=30$, 60, and 128 at 120 K. Filled circles represent the CH_3 groups.

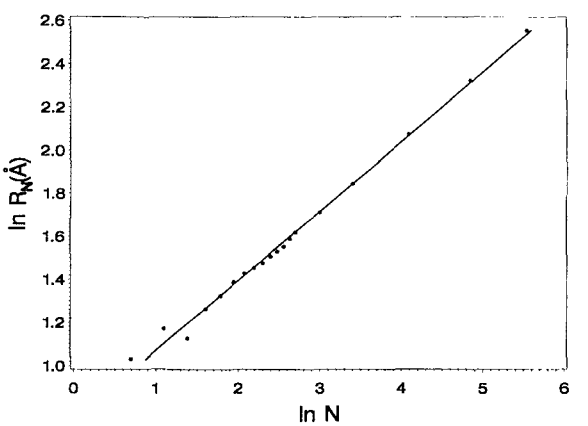

FIG. 9. Plot of $\ln R_N$ vs $\ln N$ for $[CH_3CN]_N$ at 120 K. The solid line is the least squares fit.

As indicated, we observed no evaporation from the clusters at 120 K indicating a lower vapor pressure and thus a lower relative temperature of the clusters. Recent tight-binding calculations on sodium clusters ($N=2$–34) at 0 K indicated a fractal dimension of about 3.1,[77] the same value obtained for $[CH_3CN]_N$ at 120 K. Clearly, a fractal dimension greater than 3 could result if the smaller clusters were nonspherical. Figures 4–6 suggest that the small clusters ($N \leqslant 15$) possess irregular and perhaps slightly elongated structures. Therefore, the growth pattern is from lesser compact structures to more compact (more spherical) ones. We have also observed that cold (but liquidlike) methanol clusters in this size range also have a fractal dimension around 3 (a forthcoming report),[78] and D_f values of about 3 are probably to be expected for most clusters cold enough to exist without restraining shells.

V. DENSITY PROFILES AND ORDER PARAMETERS

Density profiles giving the average number density as a function of distance from the cluster center (taken as the carbon atom of the CN group nearest the cluster center of mass) were calculated for each of the three sites (C, N, and CH_3) using spherical shells of 0.05 Å width. The results at 120 K are shown in Figs. 10(a)–10(c) along with the average density of the bulk liquid at the same temperature as represented by the horizontal dotted lines in these figures.

The results displayed in Figs. 10(a)–10(c) suggest that the cluster densities for $N=128$ and 256 more or less level out near the bulk value at about $r=8$ Å from the cluster center. The rapid convergence of the density profiles to the bulk liquid density (at 120 K) is not surprising given the low temperature involved (we have observed the same trend in methanol clusters in this size range).[79] These results are qualitatively consistent with the behavior of liquid drops composed of LJ molecules where the liquid density first rises above, then falls to the planar limit as the droplet increases in size.[80] However, the rapid convergence in the density profiles of acetonitrile clusters to the bulk liquid (at 120 K) is strikingly different from Stockmayer clusters (with vapor) where drops containing up to 896 molecules showed significantly higher liquid densities at large r than the bulk system.[81]

Another feature deserving comment in the density profiles is best observed in the N and CH_3 density profiles, where the shoulder to the right of the first peak (around 5 Å from the cluster center) begins to split off and show more structure with increasing cluster size. This splitting is most pronounced for $N=256$. This series of profiles for $N=15$–256 very much resembles the set of profiles shown by Bartell *et al.*[55] for a single cluster, $[CCl_4]_{225}$, but at several different temperatures, where the second feature in the $[CCl_4]_{225}$ density profiles becomes more structured at lower temperatures. We interpret this as indicating that the larger acetonitrile clusters are more rigid than the smaller ones. This is consistent with the decreasing heat capacities (per molecule) at larger sizes. This is also consistent with the general notion that the melting temperature decreases with decreasing cluster size, or, equivalently, that at a given temperature (below the bulk melting point) the smaller clusters may be liquidlike while the larger ones are solidlike.

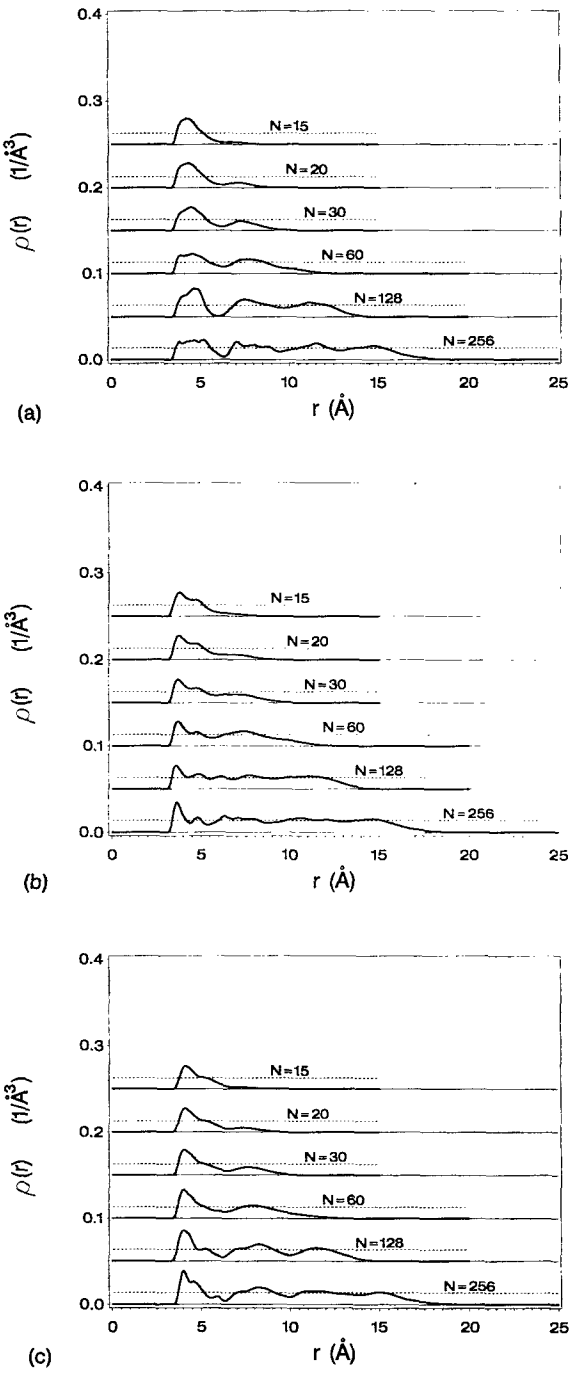

FIG. 10. (a) Carbon (CN), (b) nitrogen, and (c) methyl density profiles at 120 K for $[CH_3CN]_N$, $N=15$, 20, 30, 60, 128, and 256. Successive profiles are offset by 0.05 units on the vertical axis and the solid horizontal lines are base lines for each profile. The average bulk density at 120 K is represented by the horizontal dotted lines accompanying each profile.

Now we turn to the calculation of order parameters characterizing dipole orientation within the clusters. For molecular clusters, the density orientational profile $\rho(r,\theta)$ can be expanded in terms of Legendre polynomials $P_n(\cos\theta)$ as[81]

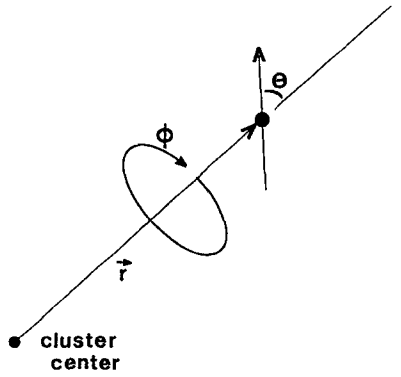

FIG. 11. Geometry for the order parameter calculation.

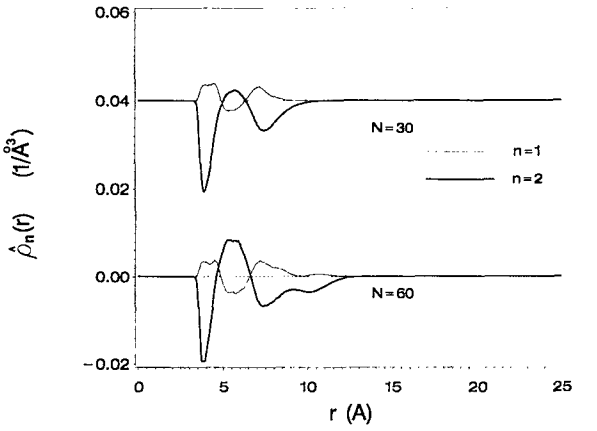

FIG. 12. First ($n=1$) and second ($n=2$) order parameters for $[CH_3CN]_{30}$ and $[CH_3CN]_{60}$ at 120 K. The $N=30$ profiles are offset by 0.04 units on the vertical axis and the dotted horizontal lines are base lines for each set.

$$\rho(r,\theta)=\sum_n \hat{\rho}_n(r)P_n(\cos\theta), \tag{5}$$

where $\hat{\rho}_n(r)$ is an order parameter and θ is the angle between the dipole vector (or a bond vector) of a molecule and its radial position vector. We define θ and ϕ as in the spherical coordinate system taking the radial position vector of each dipole to be the z axis of the spherical system, as shown in Fig. 11. The density $\rho(r,\theta)$ is given by

$$\rho(r,\theta)=\int_0^{2\pi} d\phi\ \rho(r,\theta,\phi) \tag{6}$$

and $\rho(r)$ can be obtained by integrating this over θ,

$$\rho(r)=\int_0^{\pi} \rho(r,\theta)\sin\theta\, d\theta. \tag{7}$$

We then define for each r

$$\langle P_n(\cos\theta)\rangle=\frac{\int_0^{\pi}\sin\theta\, d\theta\ \rho(r,\theta)P_n(\cos\theta)}{\int_0^{\pi}\sin\theta\, d\theta\ \rho(r,\theta)}. \tag{8}$$

Multiplying both sides of Eq. (5) by $P_n(\cos\theta)$ and integrating over θ gives

$$\hat{\rho}_n(r)=\frac{(2n+1)}{2}\int_0^{\pi}\sin\theta\, d\theta\ \rho(r,\theta)P_n(\cos\theta) \tag{9}$$

and using Eq. (8) we get

$$\hat{\rho}_n(r)=\frac{(2n+1)}{2}\rho(r)\langle P_n(\cos\theta)\rangle. \tag{10}$$

These order parameters are a measure of dipole (or bond vector) orientation relative to their radial position vectors. Near the surface of spherical clusters this is equivalent to their orientation relative to the surface normal. For this calculation an effective dipole is taken as centered on the CN carbon and parallel to the C→CH_3 bond vector.

The first and second order parameters at $T=120$ K for $[CH_3CH]_N$ with $N=30$, 60, 128, and 256 are shown in Figs. 12 and 13. The pronounced negative region in $\hat{\rho}_2(r)$ at small r is taken as an indication of the tendency for molecules to lie antiparallel to each other at short distances where the radial vector from molecule i (nearest the center-of-mass) to j will tend to be perpendicular to the dipole vector. Near the surface of the cluster another significant negative region in $\hat{\rho}_2(r)$ is observed, indicating a tendency for the dipoles to lie flat on the surface of the (spherical) cluster. This result is consistent with the findings of Shreve *et al.*[81] from a molecular dynamics study of liquid drops composed of Stockmayer molecules ($N=260$ and 896).

To illustrate the degree to which the dipoles tend to lie parallel to the cluster surface we also calculated two limiting curves for $\hat{\rho}_2(r)$ for the $[CH_3CN]_{128}$ cluster and the results are shown in Fig. 14. If all of the dipoles were oriented parallel to their radial position vectors (pointing radially outward) the upper dashed curve in Fig. 14 would have been obtained. If all of the dipoles were oriented perpendicular to the radial vector of the clusters (flat on the spherical surface), the lower dashed curve would have

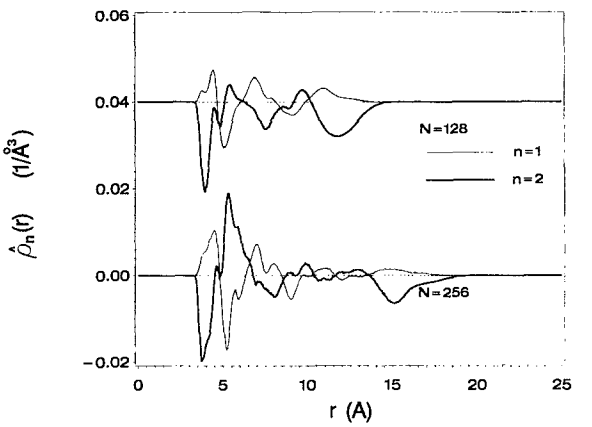

FIG. 13. First ($n=1$) and second ($n=2$) order parameters for $[CH_3CN]_{128}$ and $[CH_3CN]_{256}$ at 120 K. The $N=128$ profiles are offset by 0.04 units on the vertical axis and the dotted horizontal lines are base lines for each set.

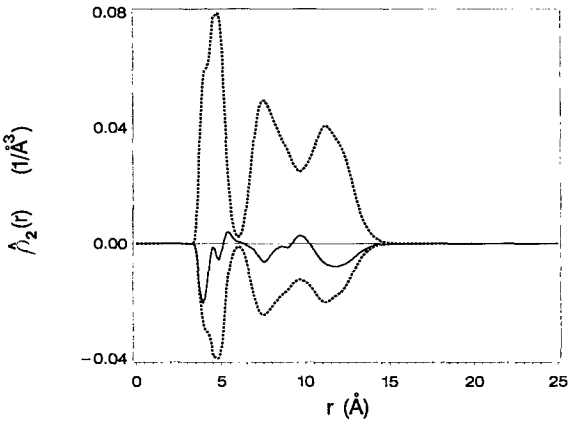

FIG. 14. $\hat{\rho}_2(r)$ for $[CH_3CN]_{128}$ at 120 K (solid line) and its limiting values. Upper dotted line for all dipoles with $\theta=0$. Lower dotted line for all dipoles with $\theta=\pi/2$.

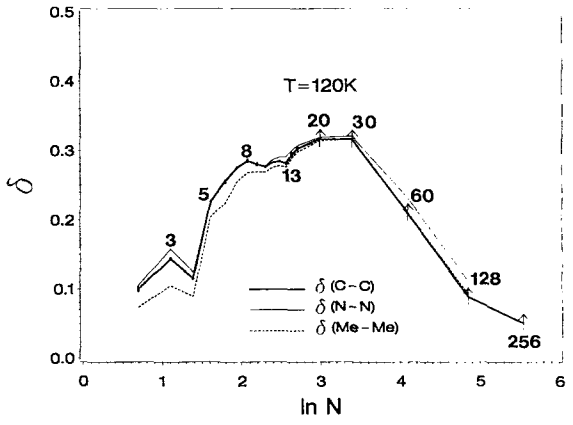

FIG. 15. The Lindemann index vs N for $[CH_3CN]_N$, $N=2$–256, at 120 K for the C_{CN}–C_{CN}, N–N, and CH_3–CH_3 site separations. Up arrows indicate lower limits.

been obtained. The simulation result (the solid line in Fig. 14) clearly indicates a net preference for alignment parallel to the cluster surface.

VI. MELTING TRANSITIONS OF SMALL CLUSTERS, $N=2$–9

In order to investigate the melting transitions we calculated the Lindemann index over a range of temperatures for the smaller clusters with $N=2$–9. This index has been used for both atomic[38,39,41,50] and molecular[48,51,56,66] clusters for the study of melting and coexistence phenomena, and is defined as the average root-mean-square fluctuation in intermolecular separation which is given by

$$\delta=\frac{2}{N(N-1)}\sum_{j>i}^{N}\frac{(\langle r_{ij}^2\rangle-\langle r_{ij}\rangle^2)^{1/2}}{\langle r_{ij}\rangle}, \tag{11}$$

where the r_{ij} are the intersite separations between two molecules. The sum in Eq. (11) should probably include only those interactions in the first coordination shell of each molecule since these are the motions that best characterize the melting process.[51] Our calculations included all r_{ij} in the sum and for the larger ($N>20$) clusters this (inappropriately) increases the value of $\langle r_{ij}\rangle$ and thus decreases the value of δ. For $N>20$ we have thus obtained lower limits for δ, which are sufficient for establishing the liquidlike nature of the clusters with $N<256$.

For atomic clusters, Lindemann's criteria for melting states that a value of $\delta<0.1$ indicates a solidlike form and a value of $\delta>0.1$ indicates a liquidlike cluster. As discussed by Bartell *et al.*,[51] the r_{ij} values in clusters of polyatomic molecules are larger than the true atom–atom contact distances. Also, molecules are typically treated as rigid particles in most MC simulations, thus neglecting intramolecular vibrations. These effects lower the threshold value of δ for molecular clusters from the value of 0.1 at which atomic clusters are considered to melt. Figure 15 displays the Lindemann indices calculated by considering the N–N, C_{CN}–C_{CN}, and CH_3–CH_3 motions for $[CH_3CN]_N$ at 120 K. The upward arrows for $N>20$ indicates that these values are to be taken as lower limits for the actual values, as explained above. At 120 K the clusters with $N<128$ are clearly liquidlike in their intermolecular motion since $\delta>0.1$ for all of these clusters, with the exception of $[CH_3CN]_2$.

Figures 16(a) and 16(b) show the Lindemann δ as a

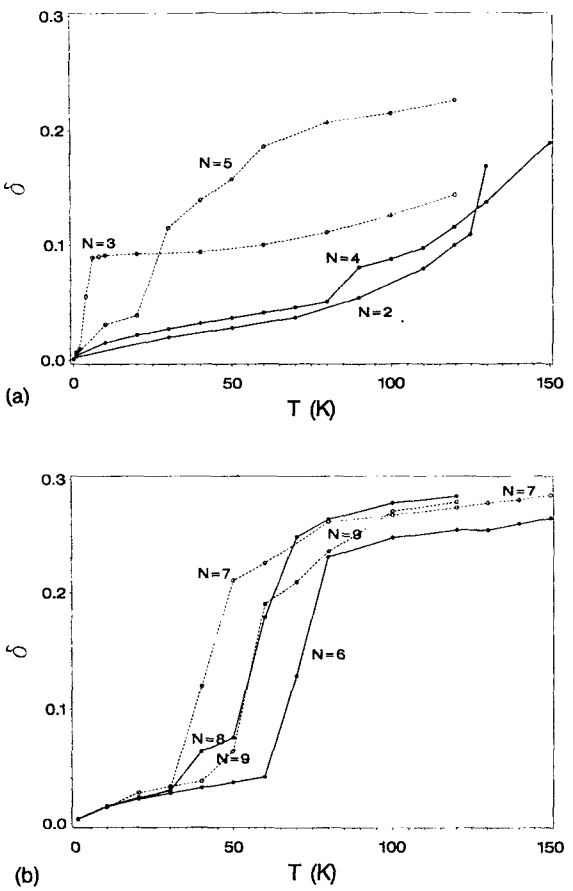

FIG. 16. The Lindemann index vs temperature for $[CH_3CN]_N$, (a) $N=2$–5 and (b) $N=6$–9, based upon the C_{CN}–C_{CN} site separations.

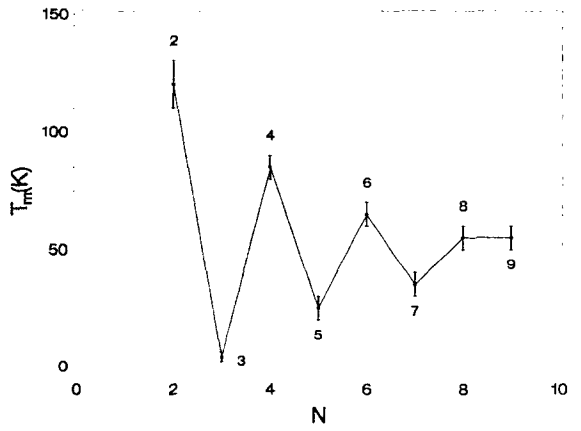

FIG. 17. Melting temperature vs N for $[CH_3CN]_N$ as obtained from the Lindemann index. The error bars were chosen to roughly encompass the melting transitions.

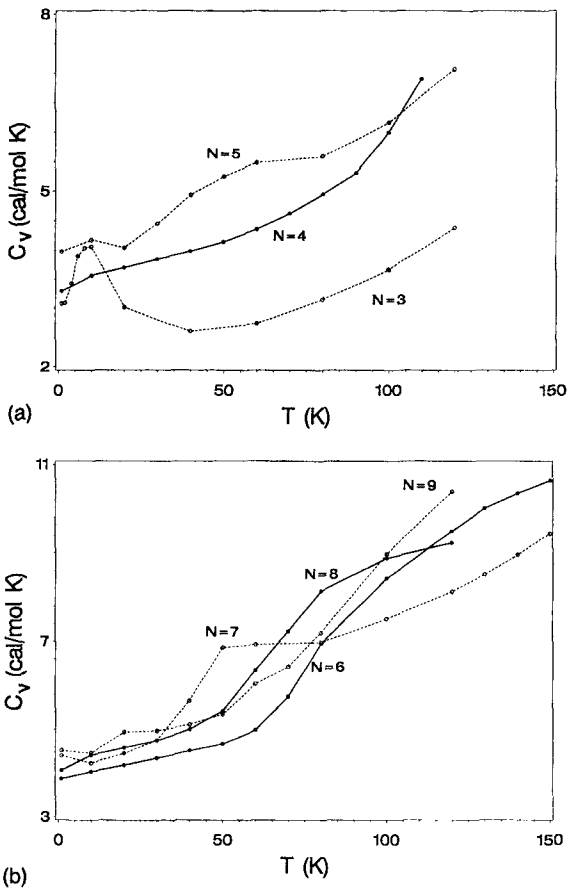

FIG. 18. Configurational heat capacity vs temperature for (a) $[CH_3CN]_N$, $N=3$–5 and (b) $[CH_3CN]_N$, $N=6$–9.

function of temperature for $[CH_3CN]_N$, $N=2$–9. For these calculations, the r_{ij} in Eq. (11) were taken as the separations between the nitrile carbons as these sites are less than 0.15 Å from the molecular centers of mass. The transitions observed in Figs. 16(a) and 16(b) suggest that small acetonitrile clusters, especially for $N=5$–9, exhibit sharply distinguishable solidlike and liquidlike forms. For the dimer, a sharp increase has been observed just before the clusters evaporated (around $T=140$ K) and this cluster may not have a well defined melting point. The trimer shows a sharp rise at very low temperatures and levels off near $\delta=0.09$–0.1. Although this cluster has not sharply crossed the 0.1 threshold value, the sharp rise at low T has been taken as indicating its phase transition. The tetramer shows a significant change of slope between 80 and 90 K, thus suggesting a phase transition, although the index values are well below 0.1. We will elaborate on this point at the end of this section.

Figure 17 exhibits a plot of the melting transition temperatures vs N and illustrates a striking even/odd alternation in this property. The even-N clusters are characterized by higher melting temperatures and more rigid structures than the odd-N clusters. However, the melting temperatures of both the even-N and odd-N series converge rather smoothly to a temperature of about 55 K at $N=8$–9. This suggests that at 55 K the clusters with $N=2$, 4, and 6 would exhibit a solidlike behavior while the clusters with $N=3$, 5, and 7 would show a liquidlike character. This unique phenomenon is apparently absent for larger clusters with $N>9$. The fact that the melting temperatures of the clusters are significantly below the bulk melting point of acetonitrile (229 K) is not surprising in view of previous results for molecular clusters of CO_2 and benzene. The small CO_2 clusters ($N=2$–7, 13) melted at temperatures lower than the bulk sublimation temperature (195 K) by more than 120 K (Ref. 56) and the benzene tetramer melted at a temperature nearly 200 K below the bulk value of 278 K.[48]

To provide further evidence for the trend observed in the melting transitions as determined from the Lindemann index, we examined the temperature dependence of the heat capacities. The results displayed in Figs. 18(a) and 18(b) confirm the even–odd alternation in the melting transitions observed from the calculation of the Lindemann index. The transition temperatures calculated from the changes in the slopes of C_v vs T are virtually the same as those obtained from the sharp rises in δ displayed in Figs. 16(a) and 16(b). This provides further evidence that melting transitions and the associated even/odd character are indeed present in small acetonitrile clusters.

This even/odd oscillation can be understood from the inspection of Fig. 19, which exhibits plots of the average percent molecules possessing an antiparallel nearest neighbor as a function of temperature for each N. The heavy line segment on each line indicates the temperature range of the transition as shown in Figs. 16(a) and 16(b). For a definition of an antiparallel dimer as $r<4.0$ Å and $160°<\theta<180°$, Fig. 19 suggests that at temperatures below the melting transitions, the $N=4$ and $N=6$ clusters are best described as clusters of dimers. Figures 20(a) and 20(b) show the structures of arbitrarily selected configurations for the $N=2$–9 clusters at 1 K, illustrating the pairing of molecules into dimers within the even-N clusters. Thus the lower transition temperatures of the $N=3$, 5, and 7 clusters can be associated with structures containing unpaired molecules.

For the $N=9$ cluster, the situation is somewhat differ-

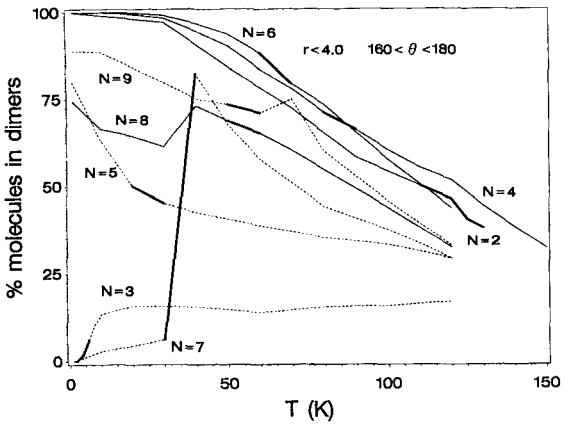

FIG. 19. Average % molecules in $[CH_3CN]_N$ having an antiparallel nearest neighbor vs T for $r_c=4.0$ Å, $\theta_c=160°$.

ent. Below the melting temperatures, the average percent of antiparallel dimers in the odd-N clusters is consistently less than in the $N-1$ (even) clusters (i.e., 3 vs 2, 5 vs 4 or 7 vs 6 in Fig. 19). However, the $N=9$ cluster shows a clear exception since at 1 K it contains about 88% (8 out of 9) molecules each possessing an antiparallel nearest neighbor compared to 75% (6 out of 8) for $N=8$. This cluster also marks the disappearance of the even/odd character observed in the energy difference (Fig. 2), the heat capacity (Fig. 3), the fraction of molecules possessing an antiparallel nearest neighbor (Fig. 8) and the melting temperature (Fig. 17). This observation leads us to suggest that the $N=9$ cluster behaves like an even cluster with respect to the melting temperature and percent molecules in dimers.

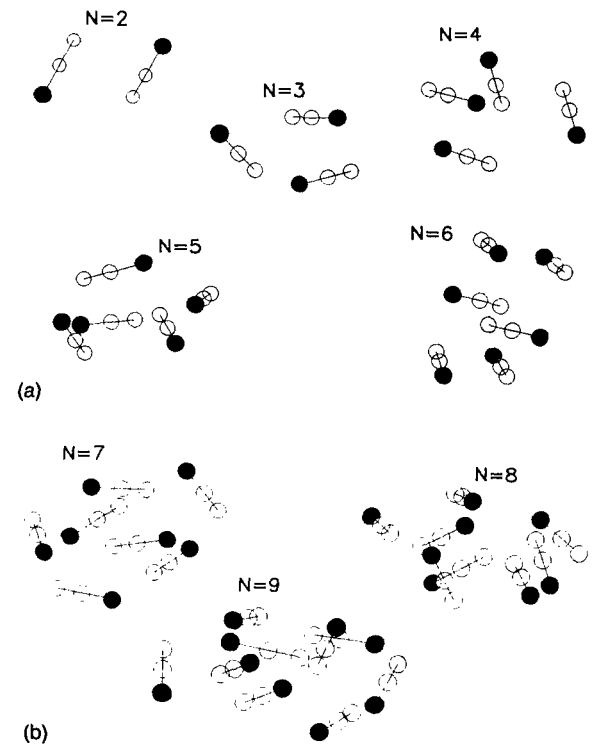

FIG. 20. Stereoplots for $[CH_3CN]_N$, (a) $N=2$–5 and (b) $N=6$–9 at $T=1$ K. Filled circles represent the CH_3 groups.

It is worth noting that Buck[25] has observed that the $N=8$ cluster exhibits spectral features similar to an odd cluster and attributed this behavior to the special stability of the $N=9$ cluster.

Another interesting consequence of paired dipoles in the even-N clusters can be seen in the melting behavior of the tetramer [Fig. 16(a)]. The increase in the Lindemann index between 80 and 90 K may indicate an increase in the relative motion between the two dimers, with the motion within each dimer remaining at values characteristic of the rigid, low temperature structure. As the calculated values of the index include all pairwise interactions, the value obtained will in a sense be an average of the lower values characteristic of the rigid dimers and more liquidlike values characteristic of the interdimer motion.

We also note that the smallest clusters ($N=2$–4) do not become fully liquidlike before they evaporate. This has also been observed for $[CH_3CN]_4$ by Al-Mubarak *et al.*[22] using the Bohm potential. Although the greater dipole moment and dimer interaction energy of the Bohm potential led to a higher melting temperature for the tetramer relative to the OPLS result, both potential models suggest that $[CH_3CN]_4$ evaporates before becoming fully liquidlike. In our calculations, δ was below 0.2 when the tetramer was observed to evaporate around 150–160 K. The OPLS potential probably underestimates the melting temperatures of the smaller clusters and it would be expected that OPLS and Bohm models give lower and upper limits, respectively, to small cluster properties that depend strongly upon dipole–dipole interaction such as the even/odd trend in energies, heat capacities, and the fraction of molecules present as dimers.

The results presented in Fig. 19 also demonstrate the unique behavior of the $(CH_3CN)_7$ cluster where, upon melting, a sharp increase in the percent molecules possessing an antiparallel nearest neighbor occurs. Thus around $T=30$–40 K the $(CH_3CN)_7$ cluster undergoes a transition from a more rigid form with essentially no pairing between molecules to a less rigid form which contains three pairs. This situation is illustrated in Fig. 21, which displays equilibrated structures of $(CH_3CN)_7$ obtained at different temperatures. It is worth noting that the structure of this cluster at 1 K resembles a distorted pentagonal bipyramid where five molecules form a cyclic planar ring capped with two additional molecules above and below the plane. This is consistent with the minimum energy structures observed with seven Lennard-Jones atoms[50] or molecules.[56]

That these effects observed in acetonitrile clusters are due to dipole–dipole interaction is also suggested by comparison with the MC study of phase transitions in small carbon dioxide clusters of Etters *et al.*,[56] where the strong tendency for parallel molecular alignments abruptly decreased during phase transitions. No such abrupt decrease is observed for the acetonitrile clusters, as indicated in Fig. 19. Also, no even–odd alternation in the transition temperatures was observed in the $(CO_2)_N$ simulations. Therefore, the even–odd alternation in the melting temperature for small acetonitrile clusters is a direct manifestation of dipole–dipole interaction. As indicated above, calculations

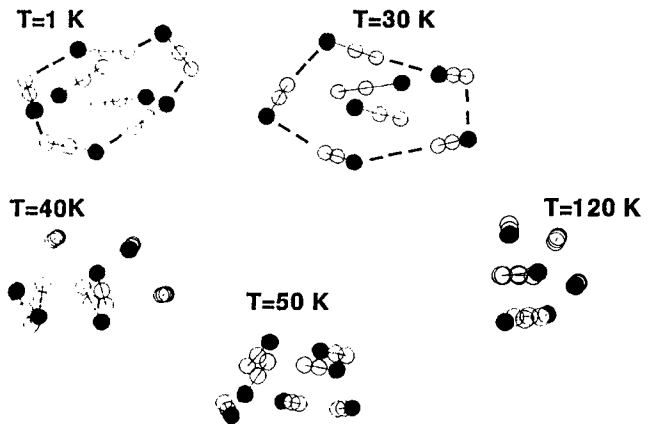

FIG. 21. Stereoplots for $[CH_3CN]_7$ at different temperatures. Filled circles represent the CH_3 groups.

with the OPLS potential model provide a lower limit for the magnitude of dipole–dipole effects and would tend to underestimate rather than overestimate these effects.

VII. CONCLUSIONS AND IMPLICATIONS FOR NUCLEATION

The simulation results suggest several novel conclusions and can provide some significant implications for the nucleation process. Consequently, the salient conclusions and implications of this study are summarized as follows.

(1) The interactions in small acetonitrile clusters are dominated by configurations in which the molecular dipoles are aligned in an antiparallel fashion.

(2) The consequences of antiparallel dipoles are clearly manifested in a remarkable even–odd character observed for the smaller clusters, including energies, heat capacities, percentage of molecules paired into antiparallel dimers and the melting transition temperatures. Convergence of the even–odd trend is observed around $N=9$.

(3) The structures of the small clusters ($N \leqslant 9$) resemble the high temperature phase of the bulk solid (216.9 $K < T < 229$ K). No evidence is found for structures resembling the low temperature solid phase which exhibits a strong tendency for head-to-head parallel alignment of molecules.[14]

(4) The average density of clusters with $N > 60$ is fairly well represented by the bulk value. This conclusion gives some support to the assumption of using the bulk liquid density for small droplets, as implied within the popular capillarity approximation, at least at lower temperatures.

(5) The order parameters for dipole orientation suggest that the dipoles tend to lie flat on the cluster surface. It should be emphasized that this result was obtained for isolated clusters (in vacuum). If this feature holds for clusters in equilibrium with the surrounding vapor molecules, then it would contradict the assumption of dipole alignments perpendicular to the surface which has been proposed to explain the slower nucleation rates observed for acetonitrile relative to the predictions of the classical nucleation theory.[26,28,79] This point requires further investigation in order to examine the structure of molecules at the interface region and to evaluate the free energies of the embryonic clusters under realistic nucleation conditions.

(6) The calculated fractal dimension and cluster structure indicate that the larger clusters (at least at 120 K) are spherical and the smaller ones have irregular shapes imposed by strong dipole–dipole interaction.

(7) The propensity of acetonitrile molecules to form antiparallel dimers could have significant implications for the kinetics of cluster growth. The classical nucleation theory assumes that clusters both grow and evaporate by gain or loss of single molecules. If the favorable dimer formation within the clusters were to lead to evaporation of molecules in dimers, this effect could enhance evaporative loss over condensation and growth. This would result in slower nucleation rates than predicted by the theory. Interestingly, recent calculations on neutral sodium clusters[77] indicate that evaporation of even-N clusters in the range of $N=4$–16 would proceed via sequential dimer loss while the odd-N clusters should evaporate by the loss of monomers.

In closing, it is hoped that our results will stimulate new experiments conducted at lower temperatures in order to elucidate in more detail the size-specific rigid $\leftrightarrow$ nonrigid transitions and the role of dipole pairings in determining the properties of clusters of highly polar molecules. Our future studies will involve a more detailed exploration of the potential surfaces and an investigation of the transition states and mechanisms for isomerization, and the coexistence behavior of these clusters.

Note added in proof: Since this work was completed, Del Mistro and Stace[82] reported a molecular dynamics study of $(CH_3CN)_N$, $N=2$–9. Their study is in complete agreement with ours regarding the even/odd trend in melting. The melting temperatures determined by the two studies differ, primarily due to the different potential functions used, as discussed in this paper. It should also be noted that the MD simulations started from the assumption of stable ordered antiparallel structures and the runs were slightly shorter than those considered necessary for melting studies of atomic clusters. In our MC study, the low temperature structures were obtained by Monte Carlo simulated annealing (MCSA) where spherical fragments of the bulk liquid at 240 K were slowly cooled to 1 K, resulting in less ordered structures than those considered in the MD study. The large number of configurations (10^8) examined in the melting study along with the small average acceptance ratio (30%) should provide sufficient accuracy to support the conclusions of our study which, in turn, support the MD results.

ACKNOWLEDGMENTS

This work was supported by the National Science Foundation Grant No. CHE-9311643. Acknowledgment is also made to the donors of the Petroleum Research Fund, administered by the American Chemical Society Grant No. 23966-G5 and to the Thomas F. and Kate Miller Jeffress Memorial Trust Grant No. J-214 for the partial support of this research. We thank Professor W. L. Jorgensen

for kindly making his MCLIQ program available and Professor J. C. Schug for valuable comments and discussions.

[1] H. Michel and E. Lippert, *Organic Liquids: Structure, Dynamics, and Chemical Properties*, edited by A. D. Buckingham, E. Lippert, and S. Bratos (Wiley, New York, 1978), Chap. 17.
[2] P. A. Steiner and W. Gordy, J. Mol. Spectrosc. **21**, 291 (1966); T. T. Bopp, J. Chem. Phys. **47**, 3621 (1967).
[3] H. Kovacs, J. Kowalewski, A. Maliniak, and P. Stilbs, J. Phys. Chem. **93**, 962 (1989); P. Yuan and M. Schwartz, J. Chem. Soc. Faraday Trans. **86**, 593 (1990).
[4] W. R. Fawcett, G. Liu, and T. E. Kessler, J. Phys. Chem. **97**, 9293 (1993); K. Kunz, P. Calmettes, and M. C. Bellissent-Funel, J. Chem. Phys. **99**, 2079 (1993).
[5] D. Smith, N. G. Adams, and E. Alge, Planet. Space Sci. **29**, 449 (1981); F. Arnold, G. Henschen, and E. E. Ferguson, *ibid.* **29**, 185 (1981).
[6] H. Bertagnolli, P. Chieux, and M. D. Zeidler, Mol. Phys. **32**, 759, 1731, (1976).
[7] H. Bertagnolli and M. D. Zeidler, Mol. Phys. **35**, 177 (1978).
[8] A. Kratochwill, J. U. Weidner, and H. Zimmermann, Ber. Bunseges. Phys. Chem. **77**, 408 (1973).
[9] T. E. Bull and J. Jonas, J. Chem. Phys. **53**, 3315 (1970); T. Tokuhiro, J. Freer, and K. H. Woo, Chem. Phys. Lett. **65**, 613 (1979); R. L. Hurle and L. A. Woolf, J. Chem. Soc. Faraday Trans. 1 **78**, 2233 (1982).
[10] W. G. Rothschild, J. Chem. Phys. **57**, 991 (1972); A. Loewenschuss and N. Yellin, Spectrochim. Acta **31**, 207 (1975); T. Bien, M. Possiel, G. Doge, J. Yarwood, and K. E. Arnold, Chem. Phys. **56**, 203 (1981).
[11] J. Schroeder, V. H. Schiemann, P. T. Sharko, and J. Jonas, J. Chem. Phys. **66**, 3215 (1977).
[12] M. Barrow, Acta Crystallogr. B **37**, 2239 (1981).
[13] E. L. Pace and L. J. Noe, J. Chem. Phys. **49**, 5317 (1968); M. P. Marzocchi and M. G. Migliorini, Spectrochim. Acta A **229**, 1643 (1973); A. Andeison and W. Y. Zeng, J. Raman Spectrosc. **17**, 447 (1986).
[14] B. H. Torrie and B. M. Powell, Mol. Phys. **75**, 613 (1992).
[15] C. S. Hsu and D. Chandler, Mol. Phys. **36**, 215 (1978); P. O. Westland and R. M. Lynden-Bell, *ibid.* **60**, 1189 (1987); R. M. Lynden-Bell and P. O. Westland, *ibid.* **61**, 1541 (1987).
[16] W. L. Jorgensen and J. M. Briggs, Mol. Phys. **63**, 547 (1988).
[17] H. J. Bohm, I. R. McDonald, and P. A. Madden, Mol. Phys. **49**, 347 (1983).
[18] H. J. Bohm, R. M. Lynden-Bell, P. A. Madden, and I. R. McDonald, Mol. Phys. **51**, 761 (1984).
[19] H. J. Bohm, C. Meissner, and R. Ahlrichs, Mol. Phys. **53**, 651 (1984).
[20] W. Langel, H. Kollhoff, and E. Knozinger, Ber. Bunsenges. Physik. Chem. **89**, 927 (1985).
[21] E. Knozinger and D. Leutloff, J. Chem. Phys. **74**, 4812 (1981).
[22] A. S. Al-Mubarak, G. Del Mistro, P. G. Lethbridge, N. Y. Abdul-Sattar, and A. J. Stace, Faraday Discuss. Chem. Soc. **86**, 209 (1988).
[23] D. J. Levandier, M. Mengel, J. McCombie, and G. Scoles, in *The Chemical Physics of Atomic and Molecular Clusters*, edited by G. Scoles (North-Holland, Amsterdam, 1990), p. 331.
[24] U. Buck, X. J. Gu, R. Krohne, and Ch. Lauenstein, Chem. Phys. Lett. **174**, 247 (1990).
[25] U. Buck, Ber. Bunsenges, Phys. Chem. **96**, 1275 (1992).
[26] D. Wright, R. Caldwell, and M. S. El-Shall, Chem. Phys. Lett. **176**, 46 (1991).
[27] D. Wright, R. Caldwell, C. Moxely, and M. S. El-Shall, J. Chem. Phys. **98**, 3356 (1993).
[28] D. Wright and M. S. El-Shall, J. Chem. Phys. **98**, 3369 (1993).
[29] H. M. Ellerby, C. L. Weakliem, and H. Reiss, J. Chem. Phys. **95**, 9209 (1991).
[30] H. M. Ellerby and H. Reiss, J. Chem. Phys. **97**, 5766 (1992).
[31] D. J. McGinty, J. Chem. Phys. **58**, 4733 (1973).
[32] J. K. Lee, J. A. Barker, and F. F. Abraham, J. Chem. Phys. **58**, 3166 (1973).
[33] C. L. Briant and J. J. Burton, J. Chem. Phys. **63**, 2045 (1975).
[34] W. D. Kristensen, E. J. Jensen, and R. M. J. Cotterill, J. Chem. Phys. **60**, 4161 (1974).
[35] R. D. Etters and J. B. Kaelberer, Phys. Rev. A **11**, 1068 (1975).
[36] R. D. Etters and J. B. Kaelberer, J. Chem. Phys. **66**, 5112 (1977).
[37] N. Quirke and P. Sheng, Chem. Phys. Lett. **110**, 63 (1984).
[38] J. Jellinek, T. L. Beck, and R. S. Berry, J. Chem. Phys. **84**, 2783 (1986).
[39] H. L. Davis, J. Jellinek, and R. S. Berry, J. Chem. Phys. **86**, 6456 (1987).
[40] J. D. Honeycutt and H. C. Andersen, J. Phys. Chem. **91**, 4950 (1987).
[41] T. L. Beck, J. Jellinek, and R. S. Berry, J. Chem. Phys. **87**, 545 (1987).
[42] T. L. Beck and R. S. Berry, J. Chem. Phys. **88**, 3910 (1988).
[43] P. Cieplak, T. P. Lybrand, and P. A. Kollman, J. Chem. Phys. **86**, 6393 (1987).
[44] J. A. Draves, Z. Luthey-Schulten, W. Liu, and J. M. Lisy, J. Chem. Phys. **93**, 4589 (1990).
[45] L. Perera and F. G. Amar, J. Chem. Phys. **93**, 4884 (1990).
[46] L. Perera and M. L. Berkowitz, J. Chem. Phys. **95**, 1954 (1991).
[47] L. Perera and M. L. Berkowitz, J. Chem. Phys. **96**, 8288 (1992).
[48] G. Del Mistro and A. J. Stace, Chem. Phys. Lett. **171**, 381 (1990).
[49] S. Weerasinghe and F. G. Amar, Z. Phys. D **20**, 167 (1991).
[50] D. J. Wales and R. S. Berry, J. Chem. Phys. **92**, 4283 (1990).
[51] L. S. Bartell, F. J. Dulles, and B. Chuko, J. Phys. Chem. **95**, 6481 (1991).
[52] M. J. Grimson, Mol. Phys. **77**, 797 (1992).
[53] F. J. Dulles, B. J. Chuko, and L. S. Bartell, in *Physics and Chemistry of Finite Systems: From Clusters to Crystals*, NATO ASI Series, edited by P. Jena, S. N. Khanna, and B. K. Rao (US GPO, Washington, DC, 1992), Vol. 374, p. 393.
[54] B. Chuko and L. S. Bartell, J. Phys. Chem. **97**, 9969 (1993).
[55] J. Chen and L. S. Bartell in Ref. 53, Vol. 374, p. 381.
[56] R. D. Etters, K. Flurchick, R. P. Pan, and V. Chandrasekharan, J. Chem. Phys. **75**, 929 (1981).
[57] F. F. Abraham, J. Chem. Phys. **61**, 1221 (1974).
[58] H. Kistenmacher, G. C. Lie, H. Popkie, and E. Clementi, Chem. Phys. **61**, 546 (1974).
[59] F. H. Stillinger and C. W. David, J. Chem. Phys. **73**, 3384 (1980).
[60] Y. J. Park, Y. K. Kang, B. J. Yoon, and M. S. Jhon, Bull. Korean Chem. Soc. **3**, 50 (1982).
[61] J. R. Reimers, R. O. Watts, and M. L. Klein, Chem. Phys. **64**, 95 (1982).
[62] G. Brink and L. Glasser, J. Phys. Chem. **88**, 3412 (1984).
[63] K. S. Kim, M. Dupois, G. C. Lie, and E. Clementi, Chem. Phys. Lett. **131**, 451 (1986).
[64] D. Belford and E. S. Campbell, J. Chem. Phys. **86**, 7013 (1987).
[65] K. Schroder, Chem. Phys. **123**, 91 (1988).
[66] D. J. Wales and I. Ohmine, J. Chem. Phys. **98**, 7245, 7257 (1993).
[67] F. T. Marchese, P. K. Mehrota, and D. L. Beveridge, J. Phys. Chem. **82**, 2497 (1978).
[68] G. Cardini, V. Schettino, and M. L. Klein, J. Chem. Phys. **90**, 4441 (1988).
[69] N. Metropolis, A. W. Rosenbluth, M. N. Rosenbluth, A. H. Teller, and E. Teller, J. Chem. Phys. **21**, 1087 (1953).
[70] M. P. Allen and D. J. Tildesley, *Computer Simulation of Liquids* (Oxford University, Oxford, 1991).
[71] W. L. Jorgensen, Chem. Phys. Lett. **92**, 405 (1982).
[72] D. M. F. Edwards, P. A. Madden, and I. R. McDonald, Mol. Phys. **51**, 1141 (1984).
[73] M. R. Hoare and P. Pal, Adv. Phys. **24**, 645 (1975).
[74] V. P. Gregory and J. C. Schug, Mol. Phys. **78**, 407 (1993).
[75] D. M. Heyes and J. R. Melrose, Mol. Phys. **66**, 1057 (1989).
[76] J. C. Schug (private communication).
[77] R. Poteau and F. Spiegelmann, J. Chem. Phys. **98**, 6540 (1993).
[78] D. Wright and M. S. El-Shall (unpublished).
[79] D. Wright, Ph.D. dissertation, Virginia Commonwealth University, July, 1993.
[80] S. M. Thompson, K. E. Gubbins, J. P. R. B. Walton, R. A. R. Chandry, and J. S. Rowlinson, J. Chem. Phys. **81**, 530 (1984).
[81] A. P. Shreve, J. P. R. B. Walton, and K. E. Gubbins, J. Chem. Phys. **85**, 2178 (1986).
[82] G. Del Mistro and A. J. Stace, J. Chem. Phys. **99**, 4656 (1993).